JCI insight

B lymphocyte alterations accompany abatacept resistance in new-onset type 1 diabetes

Peter S. Linsley, … , S. Alice Long, Matthew J. Dufort

JCI Insight. 2019;4(4):e126136. https://doi.org/10.1172/jci.insight.126136.

Research Article **Therapeutics**

Costimulatory interactions control T cell activation at sites of activated antigen-presenting cells, including B cells. Blockade of the CD28/CD80/CD86 costimulatory axis with CTLA4Ig (abatacept) is widely used to treat certain autoimmune diseases. While transiently effective in subjects with new-onset type 1 diabetes (T1D), abatacept did not induce long-lasting immune tolerance. To elucidate mechanisms limiting immune tolerance in T1D, we performed unbiased analysis of whole blood transcriptomes and targeted measurements of cell subset levels in subjects from a clinical trial of abatacept in new-onset T1D. We showed that individual subjects displayed age-related immune phenotypes ("immunotypes") at baseline, characterized by elevated levels of B cells or neutrophils, that accompanied rapid or slow progression, respectively, in both abatacept- and placebo-treated groups. A more pronounced immunotype was exhibited by a subset of subjects showing poor response (resistance) to abatacept. This resistance immunotype was characterized by a transient increase in activated B cells (one of the cell types that binds abatacept), reprogrammed costimulatory ligand gene expression, and reduced inhibition of anti-insulin antibodies. Our findings identify immunotypes in T1D subjects that are linked to the rate of disease progression, both in placebo- and abatacept-treated subjects. Furthermore, our results suggest therapeutic approaches to restore immune tolerance in T1D.

JCI insight

RESEARCH ARTICLE

B lymphocyte alterations accompany abatacept resistance in new-onset type 1 diabetes

Peter S. Linsley,[1] Carla J. Greenbaum,[2] Cate Speake,[2] S. Alice Long,[3] and Matthew J. Dufort[1]

[1]Systems Immunology Program, [2]Diabetes Program, and [3]Translational Research Program, Benaroya Research Institute at Virginia Mason, Seattle, Washington, USA.

Costimulatory interactions control T cell activation at sites of activated antigen-presenting cells, including B cells. Blockade of the CD28/CD80/CD86 costimulatory axis with CTLA4Ig (abatacept) is widely used to treat certain autoimmune diseases. While transiently effective in subjects with new-onset type 1 diabetes (T1D), abatacept did not induce long-lasting immune tolerance. To elucidate mechanisms limiting immune tolerance in T1D, we performed unbiased analysis of whole blood transcriptomes and targeted measurements of cell subset levels in subjects from a clinical trial of abatacept in new-onset T1D. We showed that individual subjects displayed age-related immune phenotypes ("immunotypes") at baseline, characterized by elevated levels of B cells or neutrophils, that accompanied rapid or slow progression, respectively, in both abatacept- and placebo-treated groups. A more pronounced immunotype was exhibited by a subset of subjects showing poor response (resistance) to abatacept. This resistance immunotype was characterized by a transient increase in activated B cells (one of the cell types that binds abatacept), reprogrammed costimulatory ligand gene expression, and reduced inhibition of anti-insulin antibodies. Our findings identify immunotypes in T1D subjects that are linked to the rate of disease progression, both in placebo- and abatacept-treated subjects. Furthermore, our results suggest therapeutic approaches to restore immune tolerance in T1D.

Introduction

The therapeutic goal for type 1 diabetes (T1D) immunotherapies is to preserve pancreatic islet β cell function, as commonly monitored by measuring insulin connecting peptide (C-peptide) levels. Several biologic therapies with distinct immunologic mechanisms of action have been tested in subjects newly diagnosed with T1D (1–7). Clinical studies with these agents have shown transient stabilization of C-peptide decline in some individuals (responders [Rs]) but not in others (nonresponders [NRs]). However, after a lag period of 6–12 months, both groups of subjects typically lose C-peptide at the same rate as control groups (2). Importantly, newly diagnosed individuals who do not receive immune-modulating therapies also show heterogeneity of C-peptide decline after clinical diagnosis (8). While heterogeneity in response to therapy and/or during natural progression has important implications for treatment of T1D, the molecular basis for this heterogeneity is currently poorly understood.

One potential route to modulating autoimmunity is blocking lymphocyte costimulatory signals. Although recognition of cognate antigenic peptides presented by MHC molecules triggers T cell receptor signaling, the engagement of T cell costimulatory receptors by ligands on antigen-presenting cells determines T cell function and fate (9). Initially, T cell costimulation was thought to provide a "second signal" for T cell activation, but currently there are more than a dozen receptor-ligand pairs known to provide costimulatory or coinhibitory signals (9). Triggering of CD28 by CD80/CD86 ligands provides a key costimulatory signal required for T cell priming (9) and helper functions (10). These interactions can be inhibited by CTLA4Ig (11), a soluble form of a CD28 homolog that has higher avidity for CD80 and CD86 counterreceptors. CTLA4Ig (abatacept) is now used widely in the treatment of immune diseases, including rheumatoid arthritis (RA) (12–14).

The clinical effectiveness of abatacept in RA prompted Type 1 Diabetes TrialNet (TrialNet) (15, 16), an international collaborative clinical trials network, to conduct a phase II trial of abatacept in new-onset

Conflict of interest: PSL received research support from Bristol-Myers Squibb and is an inventor on patent US5844095A, "CTLA4Ig fusion proteins." CJG received research support from Janssen Inc.

Submitted: November 12, 2018
Accepted: January 17, 2019
Published: February 21, 2019

Reference information:
JCI Insight. 2019;4(4):e126136.
https://doi.org/10.1172/jci.insight.126136.

T1D patients (TN-09) (3). As with some other studies of biologics in T1D (2), this study demonstrated a significant, but transient, delay in loss of C-peptide production in treated subjects, with extensive heterogeneity in response (3). To investigate mechanisms involved in response to abatacept, we applied combined systems biology and flow cytometry approaches that we have used with other T1D trials (17, 18) to studies of peripheral blood samples from the TN-09 clinical trial. Our goals were to use unbiased whole blood signatures to identify fundamental immunological mechanisms that determine response to abatacept; to compare and contrast these signatures with those seen in untreated subjects and subjects treated with other biologic agents (17, 18); and to determine how these signatures might suggest improved therapies for T1D. We observed cell signatures associated with response to T cell costimulation blockade by abatacept, most notably a signature of activated B cells, altered T cell costimulatory ligand expression, and poor pharmacodynamic activity in a subset of subjects resistant to T cell costimulation blockade.

Results

Whole blood RNA-seq analysis of T1D subjects treated with abatacept. Samples studied here came from the double-blinded study of patients with newly diagnosed T1D treated with abatacept, sponsored by TrialNet (3). In that study, subjects were randomly assigned to receive infusions of abatacept or placebo, in a 2:1 ratio, on days 1, 14, and 28 and then every 28 days, with the last dose on day 700 (n = 27 doses total). The primary outcome was the baseline-adjusted geometric mean of the 2-hour AUC serum C-peptide concentration after a mixed-meal tolerance test at the 2-year follow-up (3).

We obtained purified whole blood RNA from TrialNet and subjected these samples to RNA-seq, as described in the Methods. After quality control, we applied batch correction to the profiles to correct for different RNA preparation methods used (Supplemental Figure 1A; supplemental material available online with this article; https://doi.org/10.1172/jci.insight.126136DS1). RNA samples were not available for 7 of 112 (~6%) of the subjects originally included in the trial, but this did not significantly affect the treatment, sex, or age distribution of subjects between the original trial and the present RNA-seq studies (Supplemental Table 1).

Quantifying the rate of T1D progression using decline in C-peptide levels. Our goal was to identify gene expression signatures that identify immunological mechanisms associated with response to biologic treatment in T1D. To quantify response to treatment for gene expression comparisons, we calculated the rate of change in C-peptide loss over time in T1D patients using linear models, with patient identity as a random effect for slope and intercept and a fixed slope effect by treatment group (18, 19). Much of the variation in C-peptide decline both among subjects and over time is captured by a linear rate in log units (or exponential decay in absolute units) and resembles a first-order decay reaction (18, 19). We used these estimated rates of progression to compare subjects in the TN-09 study. Abatacept-treated subjects showed wide variation in their rates of progression (Supplemental Figure 2A). For the subjects used in our RNA-seq studies, the rate of C-peptide loss was significantly slower in abatacept- versus placebo-treated subjects (P = 0.04), consistent with the reported preservation of C-peptide levels following abatacept treatment (3). We designated abatacept-treated subjects with top-quartile rates of progression (slowest) as Rs and those in the bottom 3 quartiles in rate of progression (fastest) as NRs (Supplemental Figure 2B). When a cutoff of the same absolute value was applied to the placebo group, we found proportionally fewer R subjects (slow progressors), as would be expected with subjects that did not receive the beneficial effects of abatacept treatment.

Differences in B cell gene module expression at day 84 predict the rate of C-peptide decline in abatacept-treated patients. To identify immunological mechanisms associated with abatacept treatment, we first compared gene expression in peripheral blood of placebo- and abatacept-treated subjects. We compared profiles from subjects at different visits using gene set enrichment analysis (GSEA) (20). We employed a modular or gene-set approach for these analyses, focusing on predefined groups, or modules, of coordinately expressed and annotated genes (17, 18, 21). We compared the enrichment of modules in genes most highly expressed in placebo- and abatacept-treated subjects (Figure 1A). In contrast to our previous studies using rituximab (18), we detected no modules significantly enriched (FDR < 0.1) in abatacept-treated subjects as compared with placebo-treated subjects, at any time tested (Figure 1A). These findings were consistent with the mechanism of action of abatacept, which unlike rituximab (5) and teplizumab (4), is not known to lead to lymphocyte subset depletion following treatment (3). We then repeated the GSEA analysis, instead comparing genes ranked by expression in abatacept-treated R and NR groups (Figure 1B). None of the modules were significantly enriched in either group at the pretreatment visit (day 0), but by the day 84 visit during the

treatment period there was a group of modules significantly enriched in the NR group but not the R group (Figure 1B). These modules were no longer enriched by the day 728 visit (Figure 1B), after cessation of treatment. Prominent among the modules elevated in NR subjects were 4 overlapping modules of B cell genes (18) (Figure 1B), suggesting an increase in B cell gene expression in NR subjects. We chose one of these modules of B cell genes (CD19.mod) as a prototype for use in subsequent analyses. This module (21) comprised numerous B cell genes, including *CD19*, *CR2*, *CD79A*, *CD79B*, *CD22*, *FAM129C*, *BLNK*, *IGHD*, *IGHM*, *MS4A1*, *CD72*, *TNFRSF13C*, *BANK1*, *ICOSLG*, *CIITA*, and others.

To more directly assess the relationship between B lymphocyte gene levels and the response to abatacept, we compared median expression levels of all genes in CD19.mod with response to abatacept therapy. For these comparisons, we used both responses of R and NR as discrete variables (Figure 1C) and rate of C-peptide change as a continuous variable (Figure 1D). In the latter case, lower (more negative) values indicate faster progression and worse outcome. CD19.mod gene expression was higher in group comparisons of NR and R subjects at day 84 (Figure 1C), suggesting that during treatment B cells were elevated in the NR group, reduced in the R group, or both. CD19.mod gene expression was inversely related to rate of progression as a continuous variable (Figure 1D). In neither case was there a significant relationship between CD19.mod gene expression and rate of progression at the day 0 or day 728 visits, although there were trends in that direction at both visits. When the placebo group was tested in this fashion, the relationship between CD19.mod gene expression and rate of progression did not reach significance at any visit (data not shown). Taken together, these results suggest that modules of activated B lymphocyte genes were weakly elevated in whole blood at baseline, transiently and significantly increased during treatment, then decreased again after treatment in subjects who responded poorly to abatacept. Strikingly, this contrasts symmetrically with our previous studies in which subjects responding poorly to the B cell–depleting drug, rituximab, transiently upregulated T cell genes, which then normalized by 1 year after treatment (18).

Differences in expression of individual B cell and neutrophil genes in R and NR subjects. Analysis of expression of individual genes is a complementary approach to modular gene expression analysis and can be used to confirm and extend results obtained by modular analysis. We therefore expanded the scope of our analyses by identifying individual gene expression differences associated with abatacept treatment using linear modeling (22, 23). As we observed for modular gene expression analysis (Figure 1A), we found no individual genes showing significant differential gene expression in comparisons of abatacept- and placebo-treated patients (i.e., treatment effects) at any visit (Figure 2A and Supplemental Table 2). We next looked for individual gene expression changes associated with response in abatacept-treated subjects (i.e., comparing R versus NR groups only). Similar to the module analysis, there were few differences between groups at day 0 (Figure 2B). Differences between individual genes in the R and NR groups were greatest at the day 84 visit and then decreased again at day 728 (Figure 2B and Supplemental Table 3).

To further increase analytic power and improve our ability to detect subtle gene expression differences, we combined individual and modular module gene analyses. The central idea was that if a gene set shows no preferential association with groups of upregulated or downregulated genes, then approximately equal numbers of genes from that set would be found upregulated and downregulated. Significant group associations greater than expected by chance can be detected by enrichment analysis, even if these differences are of too low a magnitude to be detected in direct comparisons. For example, at the day 84 visit (Figure 2B), we observed that 90 of 93 CD19.mod B cell genes had log(fold-change) changes associated with NR subjects (hypergeometric $P = 2 \times 10^{-24}$). Thus, there was nonrandom association of individual B cell genes with the set of genes overexpressed in abatacept-treated subjects, even though most of them had FDR values that exceeded the significance cutoff. In contrast, neutrophil genes (MPO.mod) (21) (*ELANE, DEFA4, S100A9*, etc.) were upregulated in R subjects (74 of 84 genes, $P = 5 \times 10^{-15}$). We saw similar but weaker enrichment trends at the day 0 and day 728 visits (Figure 2B) as well as in the treatment group comparison (Figure 2A). Collectively, these findings demonstrate subtle B cell and neutrophil gene expression differences associated with NR and R groups at baseline, respectively. Moreover, differences in B cell gene expression were larger in magnitude than differences in neutrophil genes. These differences transiently increased after treatment, particularly with B cell genes, and then decreased again after treatment was stopped.

To further resolve which immune cell types were responsible for the transcriptome differences detected among abatacept-treated individuals, we compared expression of selected transcripts from R and NR profiles at the day 84 visit (Figure 2C). The B cell genes *MS4A1* (*CD20*), *CD22*, *CD19*, and *CD72* and *IGHD* levels were higher in profiles from the NR group, suggesting an elevation of B cells at a relatively mature stage

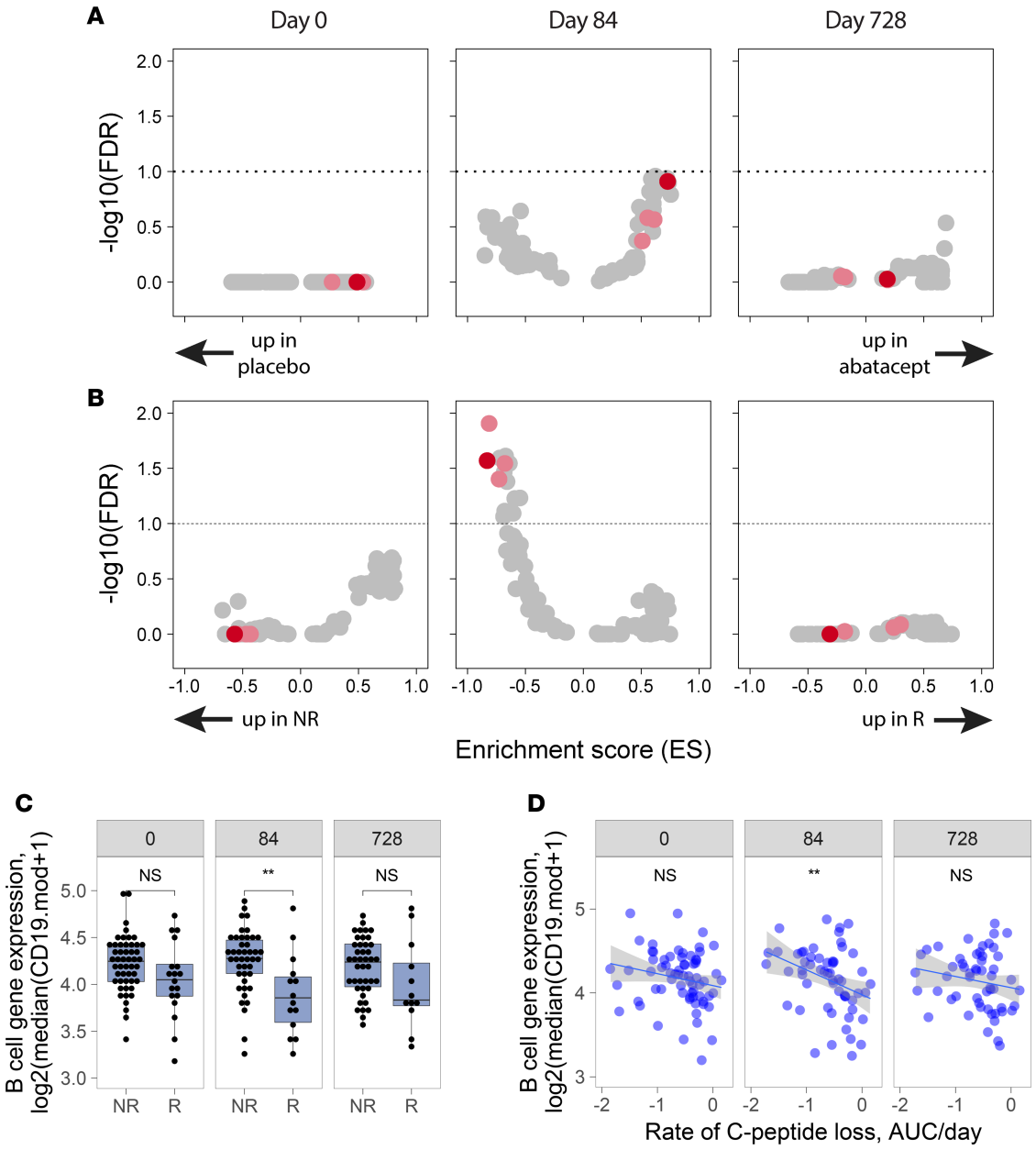

Figure 1. Abatacept treatment triggered transient changes in whole blood gene module expression. (**A**) Modular gene expression (21) analysis of abatacept- versus placebo-treated subjects using GSEA (20). Horizontal lines indicate FDR = 0.10. Red dots indicate B cell modules (n = 4); dark red dots indicate CD19.mod; gray dots indicate other gene modules (n = 107). This analysis included 69, 58, and 56 abatacept-treated subjects at the 0, 84, and 728 day visits, respectively, and 31, 30, and 27 placebo-treated subjects. (**B**) GSEA analysis of abatacept-treated R versus NR subjects. There were 51, 43, and 44 NR and 18, 15, and 12 R subjects at each visit. (**C**) B cell gene expression for abatacept-treated R and NR subjects at each visit. B cell gene expression was calculated as median [$\log_2$(CD19.mod gene RPM +1)]. Two-sided Wilcoxon P values for group comparisons are indicated. P values are presented without multiple testing correction. $^{**}P < 1 \times 10^{-2}$. (**D**) B cell gene expression for abatacept-treated subjects versus rate of C-peptide loss. P values were calculated using a linear model (B cell gene expression ~ rate of progression). Blue lines indicate slope calculated by linear model; gray shading indicates the standard error.

of development. Likewise, genes characteristic of neutrophils (and other inflammatory cells) were elevated in Rs (*DEFA3*, *IL18*, *CD14*, *CLEC12A*, and *PYCARD*). Therefore, poor response to therapy in NR subjects, characterized by fast progression, was associated with processes involving activated B cells, whereas good response to therapy in R subjects, or slow progression, was associated with neutrophils. We separately subjected the placebo group to the same analysis, using cutoffs of either the same absolute or proportional values as in the abatacept-treated group. In neither case did we observe a significant increase after treatment in differences of expression for B cell and neutrophil genes between R and NR groups of placebo subjects. This suggests that the effect sizes for regulation of these genes were smaller or more variable in the placebo

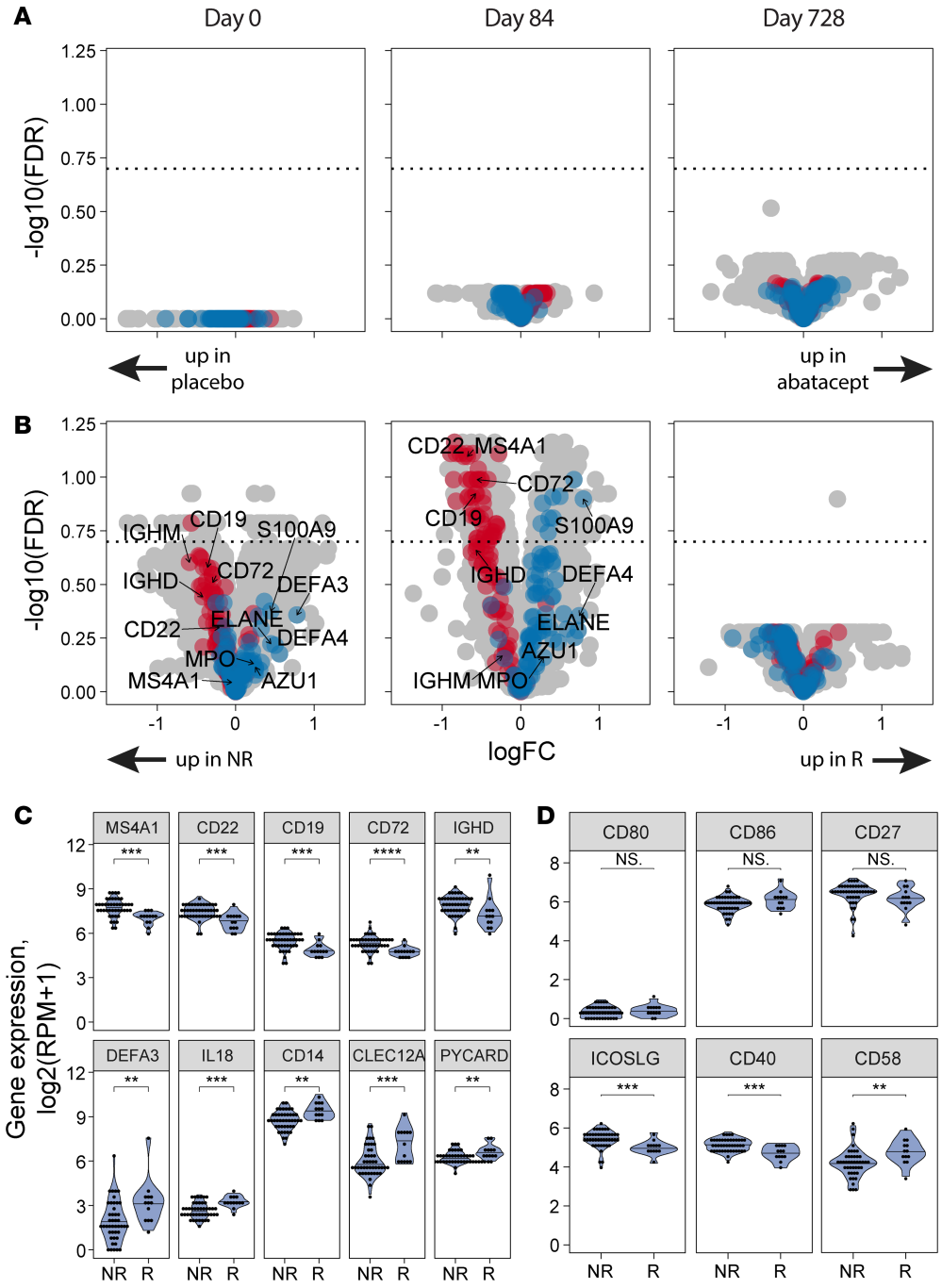

Figure 2. Gene level analysis reveals elevated B cell genes in treated NR subjects and elevated neutrophil cell genes in R subjects. (**A**) Volcano plots of individual gene expression differences between abatacept- and placebo-treated subjects calculated using a linear model implemented in limma-voom (22) (gene expression ~ treatment model). Horizontal line indicates FDR = 0.2. Red indicates B cell genes (CD19.mod); blue indicates neutrophil genes (MPO.mod). Sample numbers were as in Figure 1A. (**B**) Individual gene expression differences between R and NR abatacept-treated subjects (gene expression ~ group model). (**C**) B cell genes were enriched in abatacept-treated NR subjects, neutrophil genes in R subjects. Shown are plots of expression levels of selected B cell and neutrophil genes at the day 84 visit. Two-sided Wilcoxon *P* values for group comparisons are indicated. *P* values are presented without multiple testing correction. (**D**) Altered expression of T cell costimulatory ligands in R and NR subjects. Shown are plots of expression levels of selected T cell costimulatory ligand molecules. Molecules whose expression was not different between the R and NR groups, and molecules whose expression differed significantly between R and NR. Two-sided Wilcoxon *P* values for group comparisons are indicated. *P* values are presented without multiple testing correction. *****$P < 1 \times 10^{-5}$; ****$P > 1 \times 10^{-5}$ and $< 1 \times 10^{-4}$; ***$P > 1 \times 10^{-4}$ and $< 1 \times 10^{-3}$; **$P > 1 \times 10^{-3}$ and $< 1 \times 10^{-2}$; *$P > 1 \times 10^{-2}$ and < 0.05.

compared with the abatacept-treated group; the power of the comparison was limited by the smaller size of the placebo group or a combination of both possibilities.

One explanation for the elevated B cell gene expression associated with poor response is that it reflected an adaption to *CD28/CD80/CD86* T cell costimulation blockade. We reasoned that a potential mechanism driving such an adaptation would be altered expression of T cell costimulatory ligands. To test this, we compared gene expression of selected T cell costimulatory ligands molecules from abatacept-treated R and NR profiles at the day 84 visit (Figure 2D). *CD80* expression was very low in all samples and did not differ by response to therapy. Expression of *CD86* and *CD27* (ligand for *CD70*) also did not differ significantly in expression between the R and NR group. In contrast, *ICOSLG* and *CD40* (ligands for *ICOS* and *CD40LG*, respectively) were significantly higher in the NR group, and *CD58* (or *LFA3*, ligand for *CD2*) was significantly higher in the R group (Figure 2D). Differences in expression among *ICOSLG*, *CD40*, and *CD58* in the R versus NR groups were reduced at days 0 and 728 compared with day 84. These findings suggest a transient

reprogramming of T cell costimulatory ligand expression in response to abatacept therapy, perhaps as a mechanism of resistance to *CD80/CD86* costimulation blockade.

Biologic themes associated with expression differences in R and NR subjects. To better identify biological processes associated with gene expression differences between the R and NR groups, we performed network clustering and annotation analyses on gene modules and individual genes strongly associated with rate of C-peptide loss at peak response (day 84). Modules of B cell genes upregulated in the NR group at day 84 (Figure 1B) formed clusters of genes enriched for terms associated with B lymphocytes: B cell differentiation (*CD19*, *MS4A1* [*CD20*], *CD22*, *CD40*, etc.); B cell activation (*TCFA3*, *TCF4*, *BLNK*, *CD72*, etc.); and the Fc receptor signaling pathway (*VAV2*, *PTK2*, *PRKCE*, etc.) (Supplemental Figure 3). Individual genes upregulated in the NR group (Figure 2B) formed 3 clusters of genes enriched for terms, including "positive regulation of immune system process" (FDR = 1.9×10^{-4}; includes B cell genes, *CD22*, *CR2*, *MS4A1*, *CD40*, *CD79A*, etc.) and "chromatin modification" (FDR = 7.0×10^{-13}; *CHD7*, *SETD2*, *EP400*, etc.) (Supplemental Figure 4). In contrast, genes upregulated in R subjects (Figure 2B) were significantly annotated with GO BP terms, including "response to wounding" (FDR = 1.4×10^{-8}; *IL18*, *THBD*, *ITGAE*, *ARG1*, etc.) and "innate immune response" (FDR = 2.4×10^{-7}; *CXCL1*, *TLR2*, *CD14*, etc.). The enrichment of annotation terms in R and NR subjects was consistent with the enrichment of B cells and neutrophils in those groups following treatment.

Complex relationship between age at diagnosis, rate of progression, and response to abatacept treatment. T1D can occur at any age, but children with T1D progress more rapidly from having multiple autoantibodies to clinical disease than adults (24) and lose endogenous insulin secretion more rapidly (8). While age clearly is a factor in rate of progression of T1D, molecular mechanisms responsible for age dependence are largely unknown. During our studies, we noted that there was significant association between age at diagnosis (split at the median age, 12.8 years) with R versus NR status in abatacept-treated subjects. Specifically, 27 of 43 NR were younger than the median age, whereas 12 of 14 R were older ($P = 0.002$, Fisher's test).

To elucidate the interaction of age and response to abatacept, we compared gene expression profiles of younger and older subjects, using the combined individual gene and modular techniques described above (Figure 3A and Supplemental Table 4). Strikingly, gene expression themes associated with age (as a continuous variable) were highly similar to those associated with response/nonresponse to abatacept (Figure 2B): CD19.mod B cell genes were elevated in younger subjects, and MPO.mod genes were elevated in older subjects (hypergeometric $P = 7 \times 10^{-28}$ and 6×10^{-22}, respectively). Together, these data demonstrate a relationship between age, response to abatacept, and immune cell gene expression.

To further explore this relationship, we compared rates of progression for placebo-treated subjects and abatacept-treated R and NR subjects and assessed the association of these rates with age at diagnosis (Figure 3B). Across all subjects, rate of C-peptide loss was slower and less variable with increasing age at diagnosis. This dependence of rate of progression on age was greater in placebo- and abatacept-treated NR subjects, whereas the rate of progression for R subjects was less age dependent. Our ability to accurately assess between group differences in this analysis was limited by the small numbers of subjects tested and the extreme variation in rate of progression among subjects, particularly at younger age. However, linear modeling showed that as a group, abatacept-treated R subjects demonstrated both slower progression and less age dependence of progression compared with placebo-treated subjects ($P = 2.4 \times 10^{-4}$ and 2×10^{-2} for between group and age-group comparisons, respectively). Abatacept-treated NR subjects were intermediate between the R and placebo groups. Although younger subjects were more frequently NRs, the effects of abatacept on rate of progression (i.e., therapeutic efficacy) were also stronger in younger subjects, who presumably would have had even faster progression without treatment.

To examine how B cell and neutrophil gene expression were affected by treatment and age, we assessed median CD19.mod and MPO.mod gene expression at different study days (Supplemental Figure 5). At all visits, B cell gene expression showed an inverse relationship with age at diagnosis, with younger subjects having highest expression (Supplemental Figure 5). B cell gene expression differed most strongly among treatment groups at day 84 (Figure 3C and Supplemental Figure 5), where, in agreement with results shown in Figures 1 and 2, B cell gene expression in the NR group was elevated versus the placebo group (Figure 3C). In contrast, neutrophil gene expression showed a direct relationship with age, with older subjects having highest expression (Supplemental Figure 5). We observed no obvious trends linking R/NR status, and/or B cell gene expression, to race and/or adolescent age at onset, which were suggested in clinical studies to show variation in response to abatacept treatment (3). However, the number and/

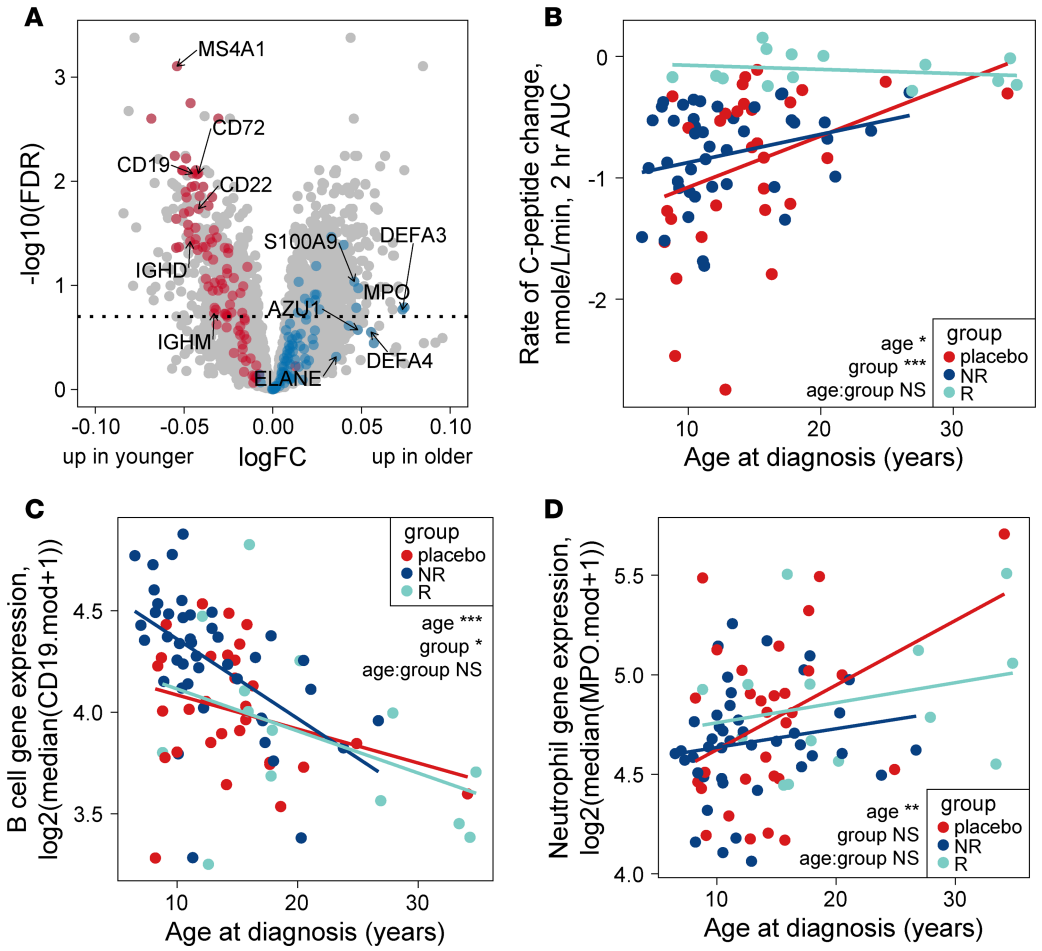

Figure 3. Covariation of age, treatment response, immune cell levels, and rate of progression. (**A**) Volcano plots of gene expression differences related to age of T1D onset (as a continuous variable) in abatacept-treated subjects (rate of progression ~ age at onset model). Plots are as in Figure 2B. Sample numbers were as in Figure 1A. (**B**) Slow progressors tend to be older at diagnosis. Shown are the rate of progression versus age at diagnosis for each subject. Comparisons between groups were determined using a linear model: rate of progression ~ age at diagnosis + group + age at diagnosis:group. This model contained fixed-effect terms for age at diagnosis and group; an interaction term for age at diagnosis and group (i.e., changes by group over age at diagnosis). *P* values for age, group, and age:group interaction terms are represented by asterisks. We obtained qualitatively similar results with more complex models. This analysis included 30 placebo-treated subjects and 43 and 14 fast and slow progressors, respectively. (**C**) Younger fast progressors express higher levels of B cell genes. Shown are the levels of B cell gene expression (median CD19.mod) at day 84 versus age at diagnosis. *P* values were determined using a linear model as in **B**. Sample numbers were as in Figure 3B. (**D**) Older slow progressors express higher levels of neutrophil genes. Shown are the levels of neutrophil gene expression (MPO.mod) at day 84 versus age at diagnosis. *P* values were determined using a linear model as in **B**. Sample numbers were as in **B**. *****$P < 1 \times 10^{-5}$; ****$P > 1 \times 10^{-5}$ and $< 1 \times 10^{-4}$; ***$P > 1 \times 10^{-4}$ and $< 1 \times 10^{-3}$; **$P > 1 \times 10^{-3}$ and $< 1 \times 10^{-2}$; *$P > 1 \times 10^{-2}$ and < 0.05.

or variation in our measurements may have limited our ability to detect such relationships. Neutrophil gene expression was consistently elevated in the placebo group at all visits (Figure 3D and Supplemental Figure 6), but this difference did not reach significance at any visit. Thus, neutrophil gene expression was slightly elevated at baseline and did not increase significantly upon treatment. Together, these findings highlight a strong reciprocal relationship between rate of progression, age at diagnosis, and B cell and neutrophil gene expression in peripheral blood. These age-related and preexisting immune phenotypes ("immunotypes") were tightly linked with rate of progression in both the untreated (placebo group) and abatacept-treated subjects. Additionally, abatacept treatment further altered B cell gene expression in NR versus R subjects, while neutrophil gene expression was less altered by treatment.

NR subjects show increased B cell counts during treatment by flow cytometry. Gene expression findings become more powerful when they can be recapitulated using different technologies. To verify the results described

above, we took advantage of complete blood count (CBC) analyses of whole blood and flow cytometry of peripheral blood mononuclear cells previously performed by TrialNet on samples from the TN-09 trial.

We first compared percentages of viable granulocytes (predominantly neutrophils), lymphocytes, and monocytes in R and NR subsets (Figure 4A), as determined by forward versus side scatter. R subjects showed significant elevations of granulocytes that did not vary with time. Complementary to this, total lymphocytes (comprising both B and T cells) were elevated in NR subjects and also did not vary with time. Monocytes were similar between groups across all time points. Flow cytometry of major immune cell types therefore supported the gene expression results, showing reciprocal alterations in neutrophil and total lymphocyte levels in R and NR subjects, respectively, throughout the course of the study. We obtained similar results with CBC measurements (Supplemental Figure 6), but the additional resolution from CBCs showed that neutrophils (as opposed to granulocytes) were elevated in R subjects. Importantly, neither light scatter nor CBC measurements allow distinction between B and T lymphocytes.

To better identify specific cell populations, we used immunofluorescence flow cytometry to determine frequencies of B cells ($CD3^-CD19^+$ lymphocytes); T cells ($CD3^+CD19^-$ lymphocytes); and monocytes ($CD3^-CD19^-CD14^+$) over time (Figure 4B). Neutrophils were not measured by immunofluorescence in these experiments. In agreement with gene expression measurements, $CD19^+$ B cell frequencies were higher at baseline in NR relative to R subjects and diverged significantly over time. By comparison, T cell levels were elevated at baseline and did not change differently over time, and monocyte levels did not differ either at the group level or over time. Thus, there was broad agreement between gene expression and flow cytometry measurements, in that there were small but consistent differences in neutrophil and B cell immunotypes linked with rate of progression. B cell levels were transiently higher in NR subjects following abatacept treatment and then normalized after cessation of treatment.

Relationship of B cell module gene expression to pharmacodynamic and mechanistic parameters from the TN-09 study. Studies in RA have shown that the ability of abatacept to inhibit autoantibody levels predicts its clinical efficacy (13, 14). We hypothesized that this occurs also in T1D and that variable efficacy of abatacept may be reflected in differential inhibition of autoantibody levels in R versus NR subjects. To test this possibility, we used levels of antibodies against several islet antigens measured during the course of the TN-09 study. We assessed levels of antibodies targeting insulin (INS, mIAA assay); receptor-type tyrosine-protein phosphatase-like N (PTPRN, IA2/ICA512 assay); and glutamic acid decarboxylase (GAD65, GAD65 assay). Antibody levels were normalized by antibody type before analysis. It is important to note that the mIAA assay is not always a measure of autoantibodies, as it cannot distinguish between insulin autoantibodies and antibodies formed de novo in response to exogenous insulin treatment (25).

We compared antibody levels between groups using linear models (Figure 5). Abatacept treatment triggered caused significant reductions in mIAA antibody levels during abatacept treatment, but levels in the abatacept-treated group converged with placebo-treated subjects after treatment ended (Figure 5A). In contrast, levels of ICA512 and GAD65 were not significantly altered by treatment, either between treatment groups or between groups over time (Figures 5, B and C). Levels of mIAA antibodies were higher in younger subjects (Figure 5D), consistent with the reported inverse correlation between age and levels of mIAA antibodies (26). In addition, levels of mIAA antibodies were strongly inhibited by treatment over time in both younger and older groups (Figure 5D). When analyzed by response to treatment groups, subjects from the placebo group had the highest levels of mIAA antibodies; miAA antibody levels were most reduced in abatacept-treated R subjects and intermediate in abatacept-treated NR subjects (Figure 5E; differences significant between response groups and between response groups over time). Finally, we examined the relationship between B cell gene expression and mIAA antibody levels (Figure 5F). B cell gene expression and mIAA antibody levels were positively correlated, and both differed significantly between groups. These results demonstrate reduced mIAA inhibition by abatacept in subjects with high B cell gene (CD19.mod) expression and suggest suboptimal pharmacodynamic activity in those individuals.

Discussion

We identified transient whole blood signatures in NR (fast progressing) abatacept-treated subjects, with a relative increase of B cell genes and decrease in neutrophil genes during treatment. We confirmed these gene expression changes using flow cytometry and CBCs. The B cell signature and cell elevation were larger in magnitude and decreased after cessation of treatment, and both had returned to baseline, or lower, after treatment. Annotation analysis showed that these B cell signatures were associated with annotation

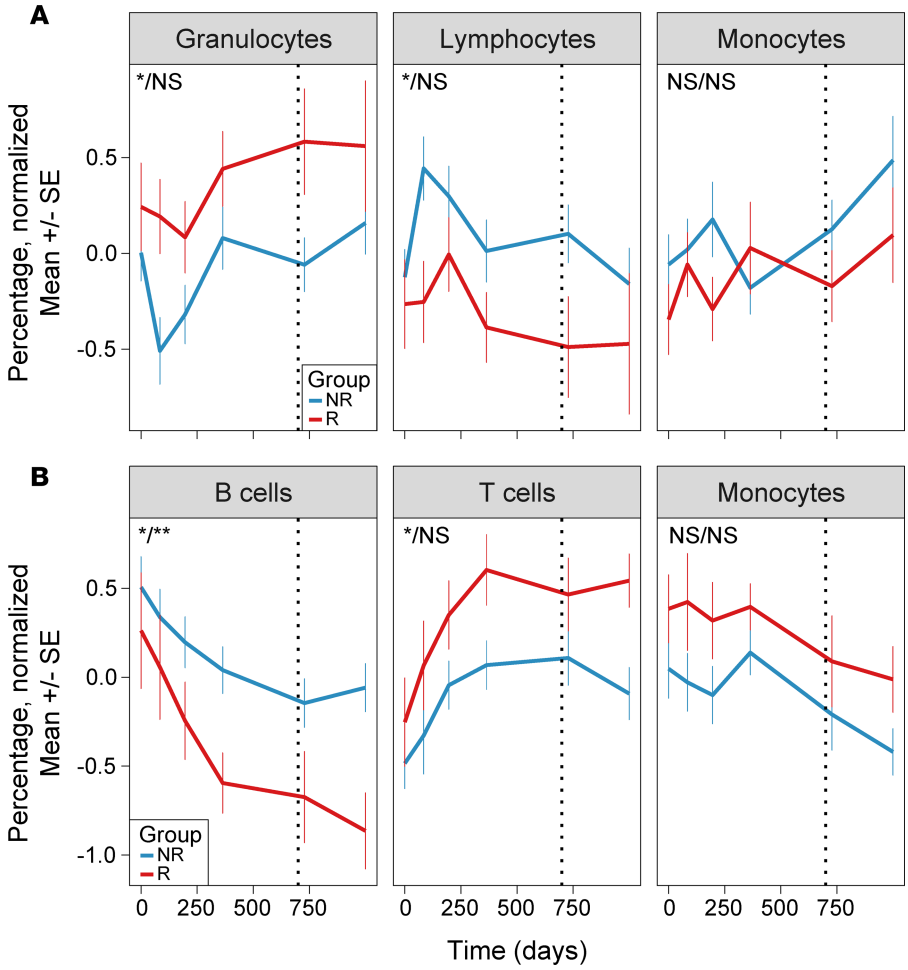

Figure 4. Flow cytometry shows that B cells and neutrophils were elevated in abatacept-treated NR and R subjects, respectively. Percentages of the indicated cell subsets determined by flow cytometry for abatacept-treated subjects were normalized by *Z* scores (value – mean of values for each subset)/(SD of values for each subset) and were plotted versus time of visit (*x* axis). The vertical dotted lines denote the day of the last dose of abatacept (day 700). Comparisons between groups were determined using a mixed-effects linear model with the lmer R package: value ~ visit + group + visit:group + (1 | id). This model contained fixed-effect terms for visit (days) and group; an interaction term for visit and group (i.e., changes in group over time); and a random effect for subject (id). *P* values determined by linear modeling and are shown as *P* values for group/*P* value for visit/group interaction. (**A**) Cell populations determined from side versus forward light scattering. Values represent viable cells determined by 7AAD dye exclusion. Mean numbers before normalization: granulocytes, 50%; lymphocytes, 43%; and monocytes, 5%. There were n = 6–17 R and n = 21–48 NR subjects at each visit. (**B**) Cell populations determined using immunofluorescence. Mean numbers before normalization: B cells (lymph/CD14$^-$/CD3$^-$/CD19$^+$), 16%; T cells (lymph/CD14$^-$/CD3$^+$/CD19$^-$), 75%; and monocytes (mono/CD3$^-$CD19$^-$/CD14$^+$), 74%. There were n = 14–19 R and n = 39–46 NR subjects at each visit. This figure is representative of 2 flow cytometry experiments that had similar results. *****$P < 1 \times 10^{-5}$; **$P < 1 \times 10^{-2}$; *$P \geq 1 \times 10^{-2}$ and < 0.05.

terms connoting B cell activation and chromatin remodeling. Coincident with the elevation in B cells, we observed altered expression of T cell costimulatory ligands *ICOSLG*, *CD40*, and *CD58* but not *CD80* or *CD86* between fast and slow progressors. Since *ICOSLG* and *CD40* are both strongly expressed on B cells, their overexpression in the NR group suggests that in these subjects there has been a reprogramming of costimulatory interactions by B cells in response to CD28/CD80/CD86 blockade. In other words, resistance to *CD28/CD80/CD86* costimulation may be mediated by accumulation of B cells that preferentially utilize *ICOS/ICOSLG* and *CD40/CD40LG* interactions in NR relative to R subjects. These alterations were reversible, and we saw few long-lasting immune alterations resulting from a 2-year course of abatacept therapy. Together, these findings showed that poor response to abatacept (resistance) in a subset of subjects was accompanied by elevations of activated B cells. It will be important to perform future studies to confirm the cellular basis for differences in costimulatory molecule expression as well as to further elucidate the mechanistic basis for how a drug that blocks T cell costimulation leads to increased B cells.

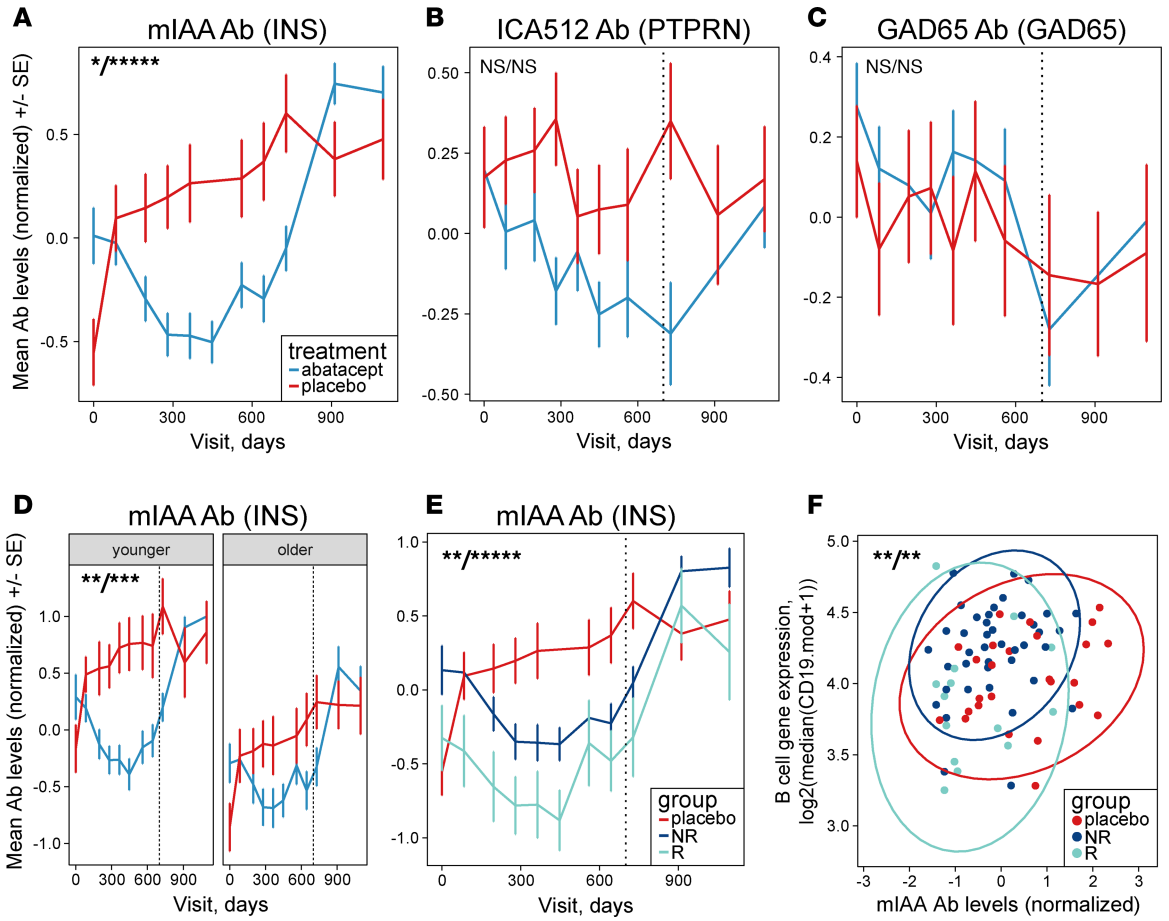

Figure 5. Faster progression and elevated B cells levels predict poor suppression of insulin antibody response. Antibodies targeting insulin (mIAA), ICA512 (IA-2), and GAD65 were measured at the indicated individual visits. Reported antibody levels were normalized using the R package bestNormalize before plotting. Shown are mean ± SEM values. (**A–C**) Treatment affects levels of mIAA, ICA512, and GAD65 antibodies. There were 55–71 abatacept-treated and 26–34 placebo-treated subjects at each visit for each of the indicated autoantibodies. The vertical dotted line denotes the day of the last does (day 700). *P* values were determined by a mixed-effect linear model on measurements made during the treatment period (i.e., <700 days): value~visit+ group + visit*group +(1|id). (**D**) This model contained fixed-effect terms for visit (days) and group; an interaction term for visit and group (i.e., changes in group over time); and a random effect for subject (id). *P* values are represented are shown as *P* values for group/*P* value for interaction. Treatment and age impact insulin antibody levels. As in **A**, except that samples from abatacept-treated subjects were further stratified according to age at diagnosis. Older, older than median age; younger, younger than or equal to median age (12.8 years). (**E**) Treatment and response to therapy impact insulin autoantibody levels. As in **A**, except that samples from abatacept-treated subject samples were further stratified according to responder status. (**F**) Differences by treatment group in the relationship between B cell gene expression and insulin antibody levels. Ellipses represent 95% confidence intervals. *P* values (p.overall) were calculated using the compareGroups R package, using a linear model: group ~ CD19.mod gene expression + antibody level model. *P* values represent the probability of group identity. *P* values are shown as *P* values for CD19.mod gene expression/*P* value for mIAA antibody levels. There were 12–19 abatacept-treated R subjects; 43–52 abatacept-treated NR subjects; and 26–34 placebo-treated subjects at each visit. *****$P < 10^{-5}$; **$P \geq 10^{-5}$ and $< 10^{-2}$; *$P \geq 10^{-2}$ and < 0.05; NS, $P > 0.05$.

Although mechanisms of abatacept blockade in vitro and in mice are reasonably well established, less is known about how the drug functions in vivo. Studies in mice have identified different T cell alterations in abatacept-treated animals (27–29). Alterations in T cell populations after abatacept treatment have also been implicated in previous human studies in RA (30, 31) and on T1D subjects from the same TN-09 trial studied here (32, 33). Orban et al. (32) reported a reduction in the CD4 central memory T cell subset in abatacept-treated subjects with slower C-peptide decline. In contrast, Cabrera et al. (33) reported positive association of baseline abundance of circulating Tregs and negative association of baseline inflammation with persistent insulin secretion. Similar in some ways to previous studies, we noted weak elevations in overall levels of T cells in R subjects by flow cytometry, but we were not able to discern which subset(s) were involved. Notably, however, we did not detect T cell alterations in our global unbiased transcriptome analyses, suggesting that these were of lower magnitude than the B cell and neutrophil differences. Taken together, the findings from our analysis, together with previous results, suggest that multiple cell types, including B cells, T cells, neutrophils, and perhaps other cell types, differ

at baseline between R and NR subjects. Further analyses may well determine that composites of immune cell types, or perhaps ratios thereof, may "predict" efficacy equally or perhaps even better than B cells or neutrophils or their transcriptome modules.

However, the strongest finding in our studies was that B cell levels changed over the course of therapy. To our knowledge this has not previously been reported, either in previous studies in T1D or in other autoimmune diseases. This may reflect differences in these previous studies and our present results, perhaps reflecting methodologies used, the particular disease setting examined, or the number of samples tested. Our studies utilized an unbiased approach and a greater fraction of the initial TrialNet abatacept trial subjects than either of the previous studies. Through C-peptide curve fitting, we also utilized a more quantitative metric for response to treatment that is less susceptible to stochastic variation between visits. We also saw greatest differences in gene expression in comparisons between response groups, rather than by treatment. Importantly, and in contrast to previous studies, we integrated multiple technologies to test predictions made using our primary methodology, gene expression measurements. Nonetheless, all of these studies were necessarily limited in power by the size of the abatacept clinical study and require validation in larger independent cohorts.

Studies of natural variation in human immune responses have led to the concept of individual immunotypes that define the state of an individual's immune system and how that individual will respond to stimuli (34). Heterogeneity in immunotypes increases with age (34). Our findings show age-related differences in both response to abatacept treatment and in the predominance of induced B cell versus neutrophil immunotypes. Since these immunotypes were detected at baseline, our findings suggest that they may contribute to age-related disease heterogeneity in T1D as well as response to abatacept. In support of this possibility, Dufort et al. (19) showed in an accompanying manuscript that similar age-related differences in baseline levels of B cell versus neutrophil immunotypes predicted the rate of loss of insulin secretion in a larger cohort of untreated new-onset T1D subjects. Other studies have reported association of B cell and/or neutrophil levels in pancreas and blood with T1D (35–39). However, since side-by-side studies in T1D and with healthy cohorts on the effects of age have not been performed, it remains unclear how much of this variation represents normal covariation with age (40). Nonetheless, these studies illustrate that appropriate patient stratification will be critical for optimal application of intervention therapies in T1D.

The overarching goal of this work was to identify molecular and/or cellular signatures in whole blood of T1D subjects responding favorably to biologic therapies and to determine whether these signatures are unique or treatment specific. Previously, we demonstrated a whole blood signature of partially exhausted $CD8^+$ T cells in patients having a favorable response to teplizumab (17). In other work (18), we showed transient elevations in expression of T cell genes associated with poor response to rituximab. Here, we show transient elevations in B cells in response to abatacept treatment. Perhaps not surprisingly, we have collectively shown that distinct molecular and cellular mechanisms are associated with beneficial response to therapy, with biologic agents having different mechanisms of action. However, with rituximab and abatacept, it was unexpected that mechanisms associated with resistance to treatment involved not the targeted cell types, but cognate partners of the targeted cell types (i.e., elevated T cells with rituximab and B cells with abatacept). Although it is important to emphasize that these correlations do not demonstrate causality, the reciprocity in these observations is intriguing.

A potential translational benefit identified here is that elevated B cell gene levels following abatacept treatment represent a candidate biomarker for efficacy of therapy. Another potential biomarker implicated in our studies is levels of insulin antibodies. Abatacept efficacy in RA has been associated with its ability to reduce autoantibody levels (13, 14). In the present studies, while ICA512 and GAD65 autoantibody levels were unaffected by abatacept treatment, mIAA levels were significantly reduced. This inhibition was greater in younger individuals and reduced in individuals with high B cell levels and poor efficacy. The differential effects of abatacept on mIAA versus other autoantibody levels may reflect previous findings that, while levels of autoantibodies to insulin are useful diagnostics prior to initiation of insulin therapy (26), antibodies targeting exogenous insulin become more prevalent after initiation of therapy (25). Moreover, abatacept is particularly effective at blocking de novo antibody responses in vivo (41). It is of interest that rituximab also affected formation of de novo antibody responses to a neoantigen (phiX174) (18, 42) and insulin (43) but not other islet autoantibodies (43). Thus, our findings suggest that inhibition of neoantigen antibodies targeting mIAA levels is a biomarker for abatacept activity in T1D.

A possible explanation for poor outcomes in subjects with high B cell levels is nonuniform pharmacodynamic activity of abatacept across different subjects. We reported a similar finding in our studies

with the rituximab trial (18). In that study, we showed that subjects with high levels of T cells showed less suppression of de novo antibodies targeting phiX174, indicating suboptimal pharmacodynamic activity of rituximab treatment. In the present study, suboptimal inhibition of mIAA antibodies in the abatacept-treated NR group also is consistent with poor pharmacodynamic activity. While inhibition of de novo antibody responses does not necessarily address immune mechanisms important for disease activity in T1D (i.e., epitope and antigen spreading, etc.), our combined results suggest that personalized dosing in individual subjects might improve efficacy of biologic agents in T1D. It is also possible that there is a relationship between increased insulin dosage, perhaps indicative of poor response to therapy, and levels of anti-insulin antibodies. While evaluating this possibility is out of the scope of the present study, it should be considered in future studies.

Another potential translational implication of our findings is their support for biologic combination therapy. A 2-year-long course of abatacept treatment in newly diagnosed T1D subjects leads to transient stabilization of β cell function, as measured by C-peptide levels, followed by a decline (3, 44). Similar findings have been seen following monotherapy with several other biologic agents (2). Our present studies show that an unintended consequence of T cell costimulation blockade by abatacept is increased levels of activated B cells that are associated with more rapid disease progression. Together with our previous studies showing that poor clinical response to B cell depletion by rituximab was accompanied by increases in T cells in peripheral blood (18), these studies recall early studies of biologic agents in organ transplantation (45). In these studies, treatment with agents that targeted either activated T cells (anti-CD40LG) or B cells (CD80 and CD86) alone showed partial effects, whereas a combination of these agents resulted in long-term graft acceptance (45). Curiously, resistance to abatacept in our experiments was accompanied by increased expression of CD40 in blood, perhaps further demonstrating the integration of these two key costimulatory systems. Taken together, the evidence suggests that it may be fruitful to test whether combination or sequential therapies of abatacept with agent(s) that block B cell activity, such anti-CD40LG or rituximab (5), more effectively restore immune tolerance to islet antigens and lead to more durable clinical effects.

Methods

Patient and sample selection. Subjects were participants in the TrialNet phase II study of the effects of the CTLA4Ig fusion protein abatacept in new-onset T1D (TN-09) (3) who had sufficient whole blood samples available for RNA preparation. Characteristics of subjects from the original trial were compared with those chosen for the current study in Supplemental Table 1. All available high-quality samples at regularly scheduled visits were utilized for each analysis. For each analysis, numbers of subjects included are indicated in the figure legends. TrialNet (https://www.trialnet.org/) also provided clinical, flow cytometry, and autoantibody data as well as 2-hour mixed-meal tolerance test results. We calculated C-peptide levels from mixed-meal tolerance test results using the R package, flux, from the trapezoidal AUC with measurements at 0, 15, 30, 60, 90, and 120 minutes. Reported autoantibody levels were normalized with the R package, bestNormalize; flow cytometry percentages were normalized by *Z* scores.

Modeling rates of C-peptide change. We estimated patient-level rates of C-peptide change over time using exponential decay using linear models fit to log-transformed C-peptide AUC measurements (18, 19). Our models included patient-level random effects terms for the intercept and slopes, with treatment as a fixed effect. We then used the patient-level coefficients from these models as a measure of the rate of T1D progression. As described previously (18, 19), this approach provided a single continuous measure of progression per patient and was tolerant of missing data from one or more visits. Our approach differed from other methods relying on fixed AUC cutoffs (4) and resembled the continuous method described by Pescovitz et al. (46).

RNA preparation from whole blood. We obtained purified whole blood RNA from TrialNet from n = 105 (71 abatacept- and 34 placebo-treated) individuals sampled at different visits (0, 84, and 728 days, ~1 month after the last dose) for an initial total of 286 samples. Whole blood was collected in Tempus tubes (Applied Biosystems). RNA was isolated from Tempus tubes using the Total RNA Isolation chemistry on ABI Prism 6100 (Applied Biosystems) or Kingfisher instruments (Thermo Fisher Scientific).

RNA-seq and pipeline analysis. We subjected samples to globin reduction with GLOBINclear kits (Ambion), and libraries were constructed from globin-reduced RNA using Illumina TruSeq RNA Sample Preparation v2 kits. Libraries were clustered on flow cells using the TruSeq Single Read Cluster Kit v3, followed by single-read sequencing for 50 cycles on a HiSeq2500 sequencer (Illumina). Pipeline processing and

alignment were as described previously (18). Individuals conducting the RNA-seq laboratory and pipeline analyses were blinded to the sample descriptions.

RNA-seq data analysis. We included high-quality RNA-seq data, defined as having more than approximately 3.2 million total reads or median coefficient of variation of read coverage of 0.4–1.0. We normalized counts using the trimmed mean of M values (TMM) (47, 48). We included genes in analyses if they had greater than 1 count per million in at least 10% of libraries. Preliminary unsupervised analysis of normalized and processed profiles by principal component analysis (PCA) revealed separation into two major clusters, particularly in the principal component 1 (PC1) dimension (Supplemental Figure 1). These clusters largely corresponded to the distribution of samples by colored by method of preparation (ABI 6100 versus Thermo Scientific Kingfisher) and by visit (day 728 versus days 0 and 84) (Supplemental Figure 1A). Consistent with the PCA plots, the distribution of samples by method of preparation differed significantly from their distribution by visit ($P < 2.2 \times 10^{-16}$) but not by treatment or R groups. To better harmonize profiles prior to analyses reported here, we performed batch correction (22) of TMM-normalized counts for method of preparation and date of RNA preparation. This correction greatly reduced the separation in PC1 by method of preparation and visit without substantially affecting distributions by treatment and R groups (Supplemental Figure 1). Importantly, we obtained qualitatively similar results when examining differences in expression of selected B cell and neutrophil genes using batch-corrected or noncorrected profiles (as in Figure 2C). Taken together, these results suggest that the batch normalization strategy did not create spurious differences for treatment or R comparisons. Unless otherwise stated, the analyses presented here utilized batch-corrected profiles.

We utilized both sex check and kinship methods to ensure that samples matched their annotation (18). Overall, we identified a total of 14 samples that were removed for poor quality ($n = 7$) or misannotation ($n = 7$). Thus, the vast majority of samples with high-quality RNA-seq profiles were consistent with subject annotation and were used in downstream analyses ($n = 272$ profiles from $n = 105$ subjects; mean of ~2.6 samples per subject) (Supplemental Table 1). We determined differential expression of individual genes with limma-voom (22). Raw *P* values were corrected for multiple testing (49). We performed gene set analyses using GSEA (20); determined PPI interactions using STRING (50) (http://string-db.org/); and visualized network graphs using Cytoscape (51) or the R package, igraph (52).

Data and code availability. Data were deposited in the GEO repository (accession GSE124284). Data files and R code are available on GitHub (https://github.com/linsleyp/Linsley_TN-09_abatacept).

Statistics. We performed all statistical tests using the R programming language and software environment (53). We fit mixed-effects models using the R package lme4 (54). Unless otherwise noted, statistical tests were 2 sided. Variances generally were assumed to be equivalent between different groups. We used *t* tests for continuous, normally distributed variables; Wilcoxon tests for nonnormally distributed variables; and Fisher's exact test for categorical variables. In all cases, we used well-established statistical tests with default settings. When parametric tests were used for plots, estimates of variation were provided. When linear models were used, models were specified in the figure legends. The specific test used to derive each *P* value is listed in the text. Graphical visualizations were performed using the ggplot2 package (55). Unless otherwise specified, we utilized 2-tailed tests; did not assume equal variance between groups; and considered a *P* value of less than 0.05 as significant.

Study approval. The TN-09 study, a parallel-group, phase II clinical trial, conformed to all applicable regulatory requirements (3). All subjects provided informed consent to participate. The study was conducted (3) under a protocol approved by the appropriate institutional review boards at each clinical study site: University of Florida, Gainesville, Florida, USA; Children's Hospital Los Angeles, Los Angeles, Californian, USA; Stanford University, Stanford, California, USA; University of Miami, Coral Gables, Florida, USA; Barbara Davis Center for Childhood Diabetes, Aurora, Colorado, USA; Joslin Diabetes Center, Boston, Massachusetts, USA; University of Minnesota, Minneapolis and Saint Paul, Minnesota, USA; Benaroya Research Institute; University of California, San Francisco, San Francisco, California, USA; University of Texas Southwestern, Dallas, Texas, USA; The Hospital for Sick Children, Toronto, Ontario, Canada; University of Pittsburgh, Pittsburgh, Pennsylvania, USA; Columbia University, New York, New York, USA; Indiana University Riley Hospital for Children, Indianapolis, Indiana, USA; and Vanderbilt Eskind Diabetes Clinic, Nashville, Tennessee, USA. The study protocol is available at the TrialNet website (https://www.diabetestrialnet.org/webapp/files/documents/protocols/TN09/04292009_1026_05%20TN09%20Pharm%20MOO%20Version%202.0%2017Feb09.pdf).

Author contributions

MJD performed analysis, assisted with data presentation, and helped prepare the manuscript. CJG and CS helped with data presentation and interpretation and preparation of the manuscript. SAL helped interpret cytometry data and with preparation of the manuscript. PSL conceived the study, performed and interpreted analysis, and prepared the manuscript.

Acknowledgments

We gratefully acknowledge the assistance and support of the TrialNet organization, especially Sarah Muller, for providing samples and clinical and demographic data. We also acknowledge Steve Nadler and Jerry Nepom for comments on the manuscript and Vivian Gersuk, Marty Timour, Kimberly O'Brien, and Quynh-Anh Nguyen for performing the RNA-seq analysis. This work was supported by a grant to PSL from the NIH (DP3 DK104465-01); funding from the Immune Tolerance Network (ITN); and NIH grant, 5UM1AI109565, awarded to Gerald T. Nepom. This work will support the mission of the ITN, which is to accelerate the clinical development of immune tolerance therapies. We acknowledge the support of the TrialNet Pathway to Prevention Study Group, which identified study participants and provided samples and follow-up data for this study. The TrialNet Pathway to Prevention Study Group is a clinical trial network funded by the NIH through the National Institute of Diabetes and Digestive and Kidney Diseases, the National Institute of Allergy and Infectious Diseases, and the Eunice Kennedy Shriver National Institute of Child Health and Human Development, through cooperative agreements U01 DK061010, U01 DK061034, U01 DK061042, U01 DK061058, U01 DK085465, U01 DK085453, U01 DK085461, U01 DK085466, U01 DK085499, U01 DK085504, U01 DK085509, U01 DK103180, U01 DK103153, U01 DK085476, U01 DK103266, U01 DK103282, U01 DK106984, U01 DK106994, U01 DK107013, U01 DK107014, and UC4 DK106993, and the JDRF. The contents of this article are solely the responsibility of the authors and do not necessarily represent the official views of the NIH.

Address correspondence to: Peter Linsley, Benaroya Research Institute at Virginia Mason, 1201 Ninth Avenue, Seattle, Washington 98101, USA. Phone: 206.818.3206; Email: plinsley@benaroyaresearch.org.

1. Rigby MR, Ehlers MR. Targeted immune interventions for type 1 diabetes: not as easy as it looks! *Curr Opin Endocrinol Diabetes Obes*. 2014;21(4):271–278.
2. Greenbaum CJ, Schatz DA, Haller MJ, Sanda S. Through the fog: recent clinical trials to preserve β-cell function in type 1 diabetes. *Diabetes*. 2012;61(6):1323–1330.
3. Orban T, et al. Co-stimulation modulation with abatacept in patients with recent-onset type 1 diabetes: a randomised, double-blind, placebo-controlled trial. *Lancet*. 2011;378(9789):412–419.
4. Herold KC, et al. Teplizumab (anti-CD3 mAb) treatment preserves C-peptide responses in patients with new-onset type 1 diabetes in a randomized controlled trial: metabolic and immunologic features at baseline identify a subgroup of responders. *Diabetes*. 2013;62(11):3766–3774.
5. Pescovitz MD, et al. Rituximab, B-lymphocyte depletion, and preservation of beta-cell function. *N Engl J Med*. 2009;361(22):2143–2152.
6. von Herrath M, Peakman M, Roep B. Progress in immune-based therapies for type 1 diabetes. *Clin Exp Immunol*. 2013;172(2):186–202.
7. Kolb H, Herrath M von. Immunotherapy for type 1 diabetes: why do current protocols not halt the underlying disease process? *Cell Metab*. 2017;25(2):233–241.
8. Greenbaum CJ, et al. Fall in C-peptide during first 2 years from diagnosis: evidence of at least two distinct phases from composite Type 1 Diabetes TrialNet data. *Diabetes*. 2012;61(8):2066–2073.
9. Chen L, Flies DB. Molecular mechanisms of T cell co-stimulation and co-inhibition. *Nat Rev Immunol*. 2013;13(4):227–242.
10. Linterman MA, et al. CD28 expression is required after T cell priming for helper T cell responses and protective immunity to infection. *Elife*. 2014;3:e03180.
11. Linsley PS, Brady W, Urnes M, Grosmaire LS, Damle NK, Ledbetter JA. CTLA-4 is a second receptor for the B cell activation antigen B7. *J Exp Med*. 1991;174(3):561–569.
12. Linsley PS, Nadler SG. The clinical utility of inhibiting CD28-mediated costimulation. *Immunol Rev*. 2009;229(1):307–321.
13. Sokolove J, et al. Impact of baseline anti-cyclic citrullinated peptide-2 antibody concentration on efficacy outcomes following treatment with subcutaneous abatacept or adalimumab: 2-year results from the AMPLE trial. *Ann Rheum Dis*. 2016;75(4):709–714.
14. Wunderlich C, Oliviera I, Figueiredo CP, Rech J, Schett G. Effects of DMARDs on citrullinated peptide autoantibody levels in RA patients-A longitudinal analysis. *Semin Arthritis Rheum*. 2017;46(6):709–714.
15. Bingley PJ, Wherrett DK, Shultz A, Rafkin LE, Atkinson MA, Greenbaum CJ. Type 1 Diabetes TrialNet: a multifaceted approach to bringing disease-modifying therapy to clinical use in type 1 diabetes. *Diabetes Care*. 2018;41(4):653–661.
16. Greenbaum CJ, et al. Strength in numbers: opportunities for enhancing the development of effective treatments for type 1 diabetes-The TrialNet Experience. *Diabetes*. 2018;67(7):1216–1225.

17. Long SA, et al. Partial exhaustion of CD8 T cells and clinical response to teplizumab in new-onset type 1 diabetes. *Sci Immunol*. 2016;1(5):eaai7793.
18. Linsley PS, et al. Elevated T cell levels in peripheral blood predict poor clinical response following rituximab treatment in new-onset type 1 diabetes [published online ahead of print June 21, 2018]. *Genes Immun*. https://doi.org/10.1038/s41435-018-0032-1.
19. Dufort MJ, Greenbaum CJ, Speake C, Linsley PS. Cell type–specific immune phenotypes predict loss of insulin secretion in new-onset type 1 diabetes. *JCI Insight*. 2019;4(4):e125556.
20. Subramanian A, et al. Gene set enrichment analysis: a knowledge-based approach for interpreting genome-wide expression profiles. *Proc Natl Acad Sci USA*. 2005;102(43):15545–15550.
21. Linsley PS, Speake C, Whalen E, Chaussabel D. Copy number loss of the interferon gene cluster in melanomas is linked to reduced T cell infiltrate and poor patient prognosis. *PLoS One*. 2014;9(10):e109760.
22. Ritchie ME et al. limma powers differential expression analyses for RNA-sequencing and microarray studies. *Nucleic Acids Res*. 2015;43(7):e47.
23. Law CW, Chen Y, Shi W, Smyth GK. Voom: precision weights unlock linear model analysis tools for RNA-seq read counts. *Genome Biol*. 2014;15(2):R29.
24. Wherrett DK, et al. Defining pathways for development of disease-modifying therapies in children with type 1 diabetes: a consensus report. *Diabetes Care*. 2015;38(10):1975–1985.
25. Radermecker RP, Renard E, Scheen AJ. Circulating insulin antibodies: influence of continuous subcutaneous or intraperitoneal insulin infusion, and impact on glucose control. *Diabetes Metab Res Rev*. 2009;25(6):491–501.
26. Vardi P et al. Concentration of insulin autoantibodies at onset of type I diabetes. *Inverse log-linear correlation with age*. 1988;11(9):736–739.
27. Patakas A et al. Abatacept inhibition of T cell priming in mice by induction of a unique transcriptional profile that reduces their ability to activate antigen-presenting cells. *Arthritis Rheumatol*. 2016;68(3):627–638.
28. Platt AM, et al. Abatacept limits breach of self-tolerance in a murine model of arthritis via effects on the generation of T follicular helper cells. *J Immunol*. 2010;185(3):1558–1567.
29. Walker LS. Treg and CTLA-4: two intertwining pathways to immune tolerance. *J Autoimmun*. 2013;45:49–57.
30. Scarsi M, et al. Reduction of peripheral blood T cells producing IFN-γ and IL-17 after therapy with abatacept for rheumatoid arthritis. *Clin Exp Rheumatol*. 2014;32(2):204–210.
31. Álvarez-Quiroga C, et al. CTLA-4-Ig therapy diminishes the frequency but enhances the function of Treg cells in patients with rheumatoid arthritis. *J Clin Immunol*. 2011;31(4):588–595.
32. Orban T, et al. Reduction in CD4 central memory T-cell subset in costimulation modulator abatacept-treated patients with recent-onset type 1 diabetes is associated with slower C-peptide decline. *Diabetes*. 2014;63(10):3449–3457.
33. Cabrera SM, et al. Innate immune activity as a predictor of persistent insulin secretion and association with responsiveness to CTLA4-Ig treatment in recent-onset type 1 diabetes. *Diabetologia*. 2018;61(11):2356–2370.
34. Kaczorowski KJ, et al. Continuous immunotypes describe human immune variation and predict diverse responses. *Proc Natl Acad Sci USA*. 2017;114(30):E6097–E6106.
35. Valle A, et al. Reduction of circulating neutrophils precedes and accompanies type 1 diabetes. *Diabetes*. 2013;62(6):2072–2077.
36. Arif S, et al. Blood and islet phenotypes indicate immunological heterogeneity in type 1 diabetes. *Diabetes*. 2014;63(11):3835–3845.
37. Diana J, et al. Crosstalk between neutrophils, B-1a cells and plasmacytoid dendritic cells initiates autoimmune diabetes. *Nat Med*. 2013;19(1):65–73.
38. Leete P, et al. Differential insulitic profiles determine the extent of β-cell destruction and the age at onset of type 1 diabetes. *Diabetes*. 2016;65(5):1362–1369.
39. Vecchio F, et al. Abnormal neutrophil signature in the blood and pancreas of presymptomatic and symptomatic type 1 diabetes. *JCI Insight*. 2018;3(18):e122146.
40. Peters MJ, et al. The transcriptional landscape of age in human peripheral blood. *Nat Commun*. 2015;6:8570.
41. Linsley PS, et al. Immunosuppression in vivo by a soluble form of the CTLA-4 T cell activation molecule. *Science*. 1992;257(5071):792–795.
42. Pescovitz MD, et al. Effect of rituximab on human in vivo antibody immune responses. *J Allergy Clin Immunol*. 2011;128(6):1295–1302.e5.
43. Yu L, et al. Rituximab selectively suppresses specific islet antibodies. *Diabetes*. 2011;60(10):2560–2565.
44. Orban T, et al. Costimulation modulation with abatacept in patients with recent-onset type 1 diabetes: follow-up 1 year after cessation of treatment. *Diabetes Care*. 2014;37(4):1069–1075.
45. Larsen CP, et al. Pillars article: long-term acceptance of skin and cardiac allografts after blocking CD40 and CD28 pathways. Nature. 1996. 381: 434-438. 1996. *J Immunol*. 2011;186(5):2693–2697.
46. Pescovitz MD, et al. B-lymphocyte depletion with rituximab and β-cell function: two-year results. *Diabetes Care*. 2014;37(2):453–459.
47. Robinson MD, Oshlack A. A scaling normalization method for differential expression analysis of RNA-seq data. *Genome Biol*. 2010;11(3):R25.
48. Robinson MD, McCarthy DJ, Smyth GK. edgeR: a Bioconductor package for differential expression analysis of digital gene expression data. *Bioinformatics*. 2010;26(1):139–140.
49. Hochberg Y, Benjamini Y. More powerful procedures for multiple significance testing. *Stat Med*. 1990;9(7):811–818.
50. Szklarczyk D et al. The STRING database in 2017: quality-controlled protein-protein association networks, made broadly accessible. *Nucleic Acids Res*. 2017;45(D1):D362–D368.
51. Shannon P et al. Cytoscape: a software environment for integrated models of biomolecular interaction networks. *Genome Res*. 2003;13(11):2498–2504.
52. Csardi G, Nepusz T. The igraph software package for complex network research. *InterJournal Complex Systems 1695*. 2006;(5):1–9.
53. R Core Team. R: A language and environment for statistical computing. R Foundation for Statistical Computing, Vienna, Austria. http://www.R-project.org/. Accessed January 23, 2019.
54. Bates D, Mächler M, Bolker B, Walker S. Fitting linear mixed-effects models using lme4. *J Stat Softw*. 2015:67(1):1–48.
55. Wickham H. *ggplot2: elegant graphics for data analysis*. New York, NY; Springer-Verlag: 2009.